Journal of Experimental Marine Biology and Ecology 449 (2013) 1–9

Contents lists available at ScienceDirect

Journal of Experimental Marine Biology and Ecology

journal homepage: www.elsevier.com/locate/jembe

A novel, non-invasive and in vivo approach to determine morphometric data in starfish

Robert Sigl [a,c,*,1], Hannes Imhof [a,c,1], Marcus Settles [b], Christian Laforsch [c]

[a] Department of Biology II, Ludwig-Maximilians-University of Munich, Großhadernerstr. 2, 82152 Martinsried, Germany
[b] Institute of Radiology, Technical University Munich, Ismaningerstr. 22, 81675 Munich, Germany
[c] Department of Animal Ecology I, University of Bayreuth, Universitätsstr. 30, 95440 Bayreuth, Germany

ARTICLE INFO

Article history:
Received 13 February 2013
Received in revised form 3 July 2013
Accepted 2 August 2013
Available online 4 September 2013

Keywords:
Acanthaster planci (Linnaeus 1758)
Echinodermata
Gonad index
Magnetic resonance imaging
Non-invasive
Pyloric cecum index

ABSTRACT

Starfish (Echinodermata: Asteroidea) are present in most benthic ocean habitats and play an important ecological role as keystone species or by dominating through sheer individual numbers. In order to assess nutritional and reproductive states in ecological studies on asteroids, invasive techniques to calculate organ indices are conventionally used. We present a non-invasive method that enables imaging and morphometric measurements in starfish in vivo. We used a clinical 1.5 T magnetic resonance imaging (MRI) scanner to produce sectional images of three starfish species and employed these image stacks to generate 3D models of the pyloric ceca, gonads and the endoskeleton. In comparison to pre-clinical MRI scanners, that provide higher resolutions, clinical MRI is not limited to small objects, but allows the investigation of larger samples such as the starfish used in the present study. Volume data from MRI-based 3D reconstructions were compared to conventional invasive measurement techniques as well as high resolution MRI scans and were tested for inter-observer effects. Here we show that MRI is a suitable method for precise imaging and volumetric measurements in fixed and living marine specimens. Compared to other methods, it allows not only the production of time series data on single individuals as well as populations, but also non-destructive analyses of valuable specimens, such as museum material.

1. Introduction

Starfish (Echinodermata: Asteroidea) are of particular importance in marine ecosystems and occupy most benthic habitats, ranging from the deep sea to the intertidal zone (Chia and Koss, 1994). Some species are regarded as keystone predators, strongly impacting community structure (Paine, 1969, 1971). Others are important for environmental management strategies due to their predatory lifestyle and regular mass outbreaks (i.e. *Acanthaster planci* (Linnaeus 1758) on coral reefs (Birkeland and Lucas, 1990); *Asterias rubens* (Linnaeus 1758) on mussel beds (Dare, 1982)). Hence, unraveling the biology and ecology of starfish has been a major challenge for marine scientists. Their slow and often cryptic lifestyle, in combination with the fact that they live in a habitat that is difficult to access has impaired research on starfish basic biology, such as their reproduction or feeding.

The determination of organ size indices taken from population subsamples constitutes a widely used tool to investigate the biology of such species. Numerous variations of these indices exist and all are obtained using invasive methods by measuring a variety of quantitative parameters of the organs or the animals themselves (for a review see Ebert et al. (2011) and Lawrence and Lane (1982)). For instance, some indices are calculated by dividing the organ's volume by the animal's wet weight (Farmanfarmaian et al., 1958). In starfish ecology, two indices are of particular importance: the gonad index (GI) and the pyloric cecum index (PCI). By following changes in the GI, the reproductive state of a starfish, and consequently the spawning season of the population, can be assessed. As starfish use a variety of reproductive strategies – some reproduce continuously and others seasonally – the reproductive timing is of particular ecological interest (Mariante et al., 2010). For instance, in *A. planci*, knowledge of the reproductive season is a key aspect in understanding patterns of successful recruitment and resulting mass outbreaks (Yasuda et al., 2010). In addition, it has been shown for several starfish species that the reproductive season depends on certain environmental gradients such as, for example, temperature (Freeman et al., 2001; Hamel and Mercier, 1995; Loosanoff, 1964). Therefore, an analysis of the reproductive state of a starfish population must be conducted separately, depending on the environmental conditions.

Apart from the gonad, another organ of starfish is of particular ecological interest, the pyloric cecum. This digestive structure is located

* Corresponding author at: Department of Animal Ecology I, University of Bayreuth, Universitätsstr. 30, 95440 Bayreuth, Germany. Tel.: +49 921 552648; fax: +49 921 552784.
E-mail address: Robert.Sigl@uni-bayreuth.de (R. Sigl).
[1] These authors contributed equally to this study.

0022-0981
http://dx.doi.org/10.1016/j.jembe.2013.08.002

pair-wise in each arm and contains storage cells, which function as the energetic reservoir of the starfish (Jangoux, 1982). In order to assess the nutritional state of a starfish, lipids can be quantified. However, decreases in these compounds during starvation do not necessarily occur. Instead, an increase or decrease in pyloric cecum size may reflect changes in the nutritional state of a starfish (Lawrence, 1973). Furthermore, pyloric ceca vary periodically in size while they follow the annual reproductive cycle of a starfish, because resources are translocated for germ cell production (Lawrence and Lane, 1982). Hence, the size of the pyloric ceca decreases, while the size of the gonads increases. Such inverse relations in the size of both organs were reported for several asteroid species (summarized by Lawrence and Lane, 1982). In contrast, some species show a simultaneous increase in the size of pyloric ceca and gonads (Lawrence, 1973). This indicates, that a direct relationship between the sizes of these two organs is not necessary.

Studies calculating organ indices using invasive methods obtain data on subsamples of the present populations. The removal of individuals from a population has often caused problems due to the sample size that is needed for statistically sound analyses. In addition, the risk of damaging local populations and of sampling artifacts increases (Menge, 1974). This is of high significance in the case of rare species or when population densities are low. However, even if densities are high, the permanent removal of large numbers of specimens from a local population may interfere with inter- and intraspecific interactions and is, especially for ecological questions, problematic (Menge, 1972; Turk et al., 1978). Another problem of invasive techniques is that they do not allow tracking of organ size changes over time in a single individual. This limitation prevents a deeper insight into the ecology of organ size variation and the ontogeny of organs. To overcome this restriction, non-lethal and non-invasive methods are needed (Boistel et al., 2011). A method that does not involve euthanizing the animal, while using the regenerative potential of most starfish, was introduced by Sanford et al. (2009), who found that sampling of only one arm in the starfish *Pisaster ochraceus* (Brandt, 1835) can be used to determine organ indices. Although this method is non-lethal, it still has the limitation that it cannot be applied in time series studies.

The application of modern imaging techniques and computerized 3D reconstruction to obtain quantitative data on animals has shown potential to fill this void. These methodologies have therefore become a sophisticated tool in organismal biology (e.g. Laforsch et al., 2012). For example, by using 3D models derived from computed tomography (CT) scans, the surface area of living stony corals (Cnidaria: Scleractinia) can be estimated (Kaandorp et al., 2005; Laforsch et al., 2008). In contrast to hard part imaging using CT, magnetic resonance imaging (MRI) has demonstrated its applicability for imaging soft part anatomy of a wide range of animal taxa (for a review see Ziegler et al. (2011)). Based on the principles of nuclear magnetic resonance, MRI scanners detect primary hydrogen protons. Exposed to a strong magnetic field, the nuclear magnetic moments of the protons form a so-called longitudinal magnetization parallel to the external magnetic field. Using radio-frequency pulses, this longitudinal magnetization is tilted into the plane perpendicular to the magnetic field forming a so-called transverse magnetization. The latter rotates about the direction of the magnetic field while being a magnetic field itself and induces an alternating electric current in a receiver coil. This magnetic resonance signal is then used for imaging by translating it into gray-value cross-sectional images consisting of volumetric pixels (voxels). MR imaging always requires some sort of compromise between parameters that affect spatial resolution, image quality and scan duration on one hand and the susceptibility to artifacts (e.g. image distortion due to agents that affect the uniformity of the static magnetic field) on the other. Concerning the latter aspect, for anatomic imaging one generally prefers spin echo sequences or rather their fast variant turbo spin echo (TSE) or fast spin echo (FSE) (different acronyms used by different scanner manufacturers) to minimize distortive artifacts. With this technique a high spatial resolution (meaning well below 1 mm in all three spatial directions) can be achieved only with long scan times of several hours on a 1.5 T clinical scanner. As this is not feasible with living specimens one switches to a sequence type which, due to its intrinsically higher signal intensity at short time scales, allows for a fairly high resolution (still sub-millimeter), but within a scan duration of well below 1 h ($\approx$15 min). This sequence is a gradient echo variant called balanced fast field echo (bFFE), trueFisp or FIESTA (again different manufacturers) but with the drawback of an increased susceptibility to the distortive effects of metal, calcifications or air bubbles. In addition to the imaging itself, the processing of image stacks obtained by visualization techniques is already well developed and a wide palette of proprietary and free 3D modeling software exists.

This study introduces MRI-based computerized 3D modeling as a novel, in vivo, and non-invasive method to obtain morphometric data from starfish. To minimize the stress experienced by living starfish, it is crucial to reduce the MRI scan time to a minimum. Because spatial resolution is one of the factors largely influencing scan time we tested for differences in volumetric data obtained from 3D models when scanning in high resolution and low-resolution mode. Additionally, we compared volumetric data obtained using our approach with data derived from the invasive liquid displacement method.

2. Materials and methods

In general, our approach involves three steps to obtain morphometric data from starfish. First, the starfish is scanned using MRI. Second, the MRI image stack obtained is processed to create 3D models of the structures of interest. Third, the volumes of these 3D models are calculated. In order to reduce the use of animals we developed the workflow using preserved specimens of *A. planci* (Linnaeus, 1758) and subsequently tested the general applicability of our approach in three living starfish species (*A. planci*, *Culcita novaeguineae* (Müller and Troschel, 1842), *Pentaceraster alveolatus* (Perrier, 1875)). Inter-observer variability was tested using untrained persons that applied the method to MRI image data derived from a single living specimen of *A. planci*.

2.1. MRI of preserved specimens

For the initial imaging trials and later image processing, five *A. planci*, ranging in diameter (arm tip to arm tip) from 17.4 cm to 22.9 cm, were obtained from the University of Guam Marine Laboratory (Mangilao, Guam, USA). Three specimens were preserved and stored in 70% ethanol and two were preserved in 10% formalin in seawater and stored in 70% ethanol. For MRI, the starfish were placed into a closed plastic container (27.5 cm × 22 cm × 8 cm) filled with approximately 3 l of 70% ethanol. The size of the plastic container was chosen so that the receiver coil could be placed as close as possible to the scanned starfish in order to achieve sufficient signal-to-noise ratio. One arm of the starfish was marked using a rubber band in order to permit orientation and correct comparison of organs in single arms or interradia. The preserved specimens of *A. planci* were scanned using a Philips Achieva 1.5 T clinical MRI system (Philips Healthcare, Eindhoven, The Netherlands). A SENSE receiver coil for cardiac imaging and a T2-weighted 3D turbo spin echo (3D-TSE) scanning sequence were employed. Due to artifacts caused by air bubbles trapped inside the body cavity the scanning sequence for the preserved specimens varied from that used for living specimens (3D balanced fast field echo; see Section 2.4). Both high-resolution (0.0063–0.0135 mm^3/voxel) and low-resolution (0.082–0.098 mm^3/voxel) scans were performed in order to test for any influence of the adjusted resolution on the accuracy of MRI-derived volume data. The following parameters were adjusted for high- and low-resolution scans, respectively: acquisition time (T_A) 10–19.6 h or 12–25 min; repetition time (T_r) 1000 ms or 750 ms; and echo time (T_E) 81–97 ms or 78–79 ms. Flip angle was 90°, while field of view dimensions varied depending on the size of the starfish.

2.2. 3D reconstruction

The image stacks were processed using the software package Amira 5.2.2 (Visage Imaging GmbH, Berlin, Germany). No further adjustment or alteration of the images was needed as the dataset is obtained in medical standard DICOM-format and images are already aligned to stacks. Five to seven arms of each starfish were chosen for 3D reconstruction of the gonads and the pyloric ceca. In every arm, both strings of the pyloric ceca were used as a single unit for reconstruction. The pyloric ceca were reconstructed from the distal tip to the point where both strings merge together into the pyloric duct leading to the pyloric stomach. Furthermore, the gonads on both sides of the interradial septum were fused into a single unit for reconstruction. Segmentation was performed in each sectional image, first in the horizontal plane and then revised in two different vertical, orthogonal sectional planes as well as in the 3D view. The segmentation workflow was to i) draw a "limit-line" around the specific organ, ii) use the "magic wand" tool to choose an appropriate gray-scale threshold that marked the structure of interest, and iii) to correct the marked area with the "brush" or "lasso" tool for parts not counting to the specific organ. To produce a 3D model of the entire starfish, the body was segmented by selecting all voxels with appropriate gray-scale values for skeletal elements (i.e. black). Volumetric data for organs were calculated using the amount of segmented voxels for every single unit of reconstruction. These data were obtained using the "material statistics" function and the voxel size values deposited in the DICOM file header. For visualization of the reconstructed organs, the "surface-gen" module in Amira 5.2.2 was used with options "non-smoothing" as well as "compactify" activated and the option "add border" deactivated.

2.3. Volume calculation of organs using the method of liquid displacement

In order to test our approach for comparability with conventional methods, the MRI-derived volumetric data were compared to volumetric data obtained by liquid displacement (Mauzey, 1966). After data acquisition using MRI, the five preserved specimens were dissected in air and the respective organs were extracted. The pyloric ceca were cut proximate to the pyloric stomach at the pyloric duct. Gonads were extracted by gentle removal from the interradial septum. All organs were stored in a 30 ml snap-cap vial in alcoholic atmosphere (70% ethanol) after extraction. The organs were measured in 70% ethanol using a 10 ml graduated cylinder with ± 0.1 ml error margin (Duran Group GmbH, Wertheim/Main, Germany). A sufficient amount of ethanol was added to the cylinder and the liquid level was noted. In the next step organs were drained and transferred into the cylinder using forceps and the new liquid level was noted as follows: if the meniscus was exactly in the middle of two calibration marks (0.2 ml steps), the value was read as 0.1 ml. Otherwise, the value to the closest calibration mark was noted. The difference between the two levels was calculated to determine the organ volume.

2.4. In vivo MRI

In order to test the applicability of our approach to other starfish, one living specimen of three additional starfish species (*A. planci*, *P. alveolata*, *C. novaeguineae*) was taken from the coral reef aquaria located at the Department of Biology II, LMU Munich, Germany and scanned using MRI. For scanning, the starfish were anesthetized using a 3.5% magnesium chloride hexahydrate ($MgCl_2 \times 6H_2O$) solution in demineralized water. This solution was then mixed with seawater from the aquarium to reduce the concentration of $MgCl_2 \times 6H_2O$ in the medium to 2.5%. In preliminary experiments this concentration proved to be the optimal compromise between the shortest amount of time required for starfish relaxation and the fastest recovery time of the animal when placed back into seawater. Furthermore, this medium did not alter the salinity of the water, thus avoiding osmotic stress for the starfish. For scanning, the starfish were placed into a plastic container (27.5 cm × 22 cm × 8 cm) filled with approximately 3 l of the anesthetic–seawater mixture. The same MRI scanner and receiver coil were used as for preserved specimens. A 3D balanced fast field echo sequence (3D-bFFE) was applied for scanning (0.098 mm^3/voxel; T_A 15–19 min; T_R 7.7 ms; T_E 3.85 ms; flip angle 45°). 3D reconstruction was accomplished as for the preserved starfish.

2.5. Test for inter-observer variability

In order to test for possible observer effects in the volumetric data from 3D reconstructions, five independent, untrained persons reconstructed gonads and pyloric ceca of the same five arms of a single specimen of *A. planci* scanned in vivo. A T2-weighted 3D turbo spin echo (3D-TSE) was used. One arm of the starfish was marked by fixing a cable tie around a spine to assure correct comparisons of obtained volumetric data. The procedure and equipment used for scanning and 3D reconstruction were the same as for all other experiments. The test was performed blind and all observers were students briefly introduced into the use of the software Amira 5.2.2.

2.6. Statistical analyses

All statistical analyses were performed using the software SPSS Statistics 19.0.0 (SPSS, Inc., Chicago, IL, USA). The standard error of mean was used to compare the data. In order to test for the agreement of volumes determined using low-resolution and high-resolution scans as well as low-resolution scans and liquid displacement method the "95% limits of agreement" method from clinical measurement comparisons (Bland and Altman, 1986, 2003) was applied. By calculating the mean difference (measure of the offset) and the 95% confidence interval, limits of agreement were created that depicted 95% of all differences (Matre et al., 1999). The t-factors for the 95% confidence interval were adapted to the sample size (Hayek and Buzas, 2010). The normal distribution of the differences was tested using a Kolmogorov–Smirnov test.

3. Results

3.1. MRI of preserved specimens

High-resolution MRI data obtained from preserved specimens of *A. planci* showed detailed internal organization. Image resolution, gray-scale values, and textures allowed for the identification of various structures inside the body cavity, such as pyloric ceca, gonads, skeletal elements, tube feet, ampullae and Polian vesicles (Fig. 1A). However, specimens conserved in 70% ethanol contained small air bubbles (Fig. 1A). In contrast, formalin-fixed specimens were well preserved and organs were in a natural shape. Low-resolution scans displayed fewer details than high-resolution scans, but all organs as well as skeletal elements could nonetheless be differentiated (Fig. 1B).

3.2. Comparison of volumetric datasets

The volumetric data as well as the differences calculated for comparison of the different methods were distributed normally (Kolmogorov–Smirnov-test: p = all not significant). The mean volume of the pyloric ceca was higher when using the liquid displacement method compared to the volume obtained in either the high-resolution or the low-resolution MRI scans (Table 1). In contrast, the highest mean volume for the gonads was measured based on high-resolution scans. For both organs, high-resolution scans resulted in slightly higher volume data than low-resolution scans (Table 1). The mean error (i.e. mean difference) for all comparisons between two methods and organs – except those for the pyloric ceca in the low-resolution scans vs. liquid displacement method comparison – was below 0.1 cm^3 (Table 2). The highest difference was found in the comparison between the volumes of the

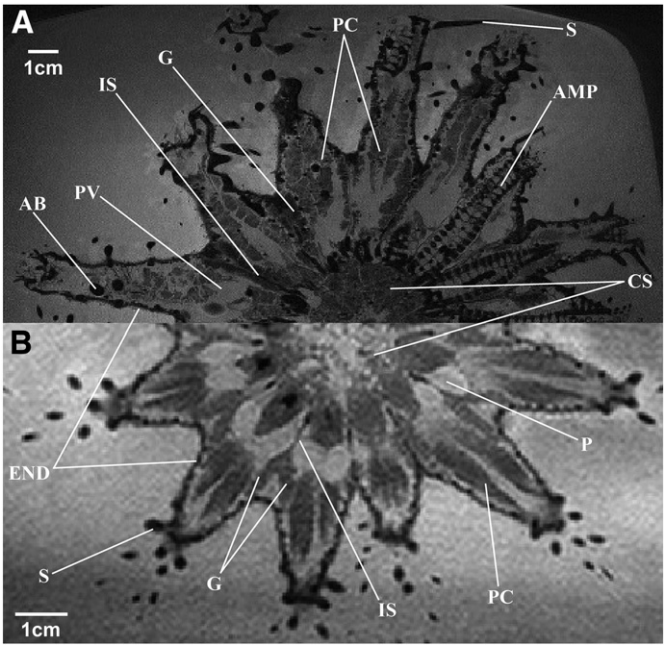

Fig. 1. (A) Half cross-sectional image based on a high-resolution MRI scan of a preserved specimen of *A. planci* scanned in 70% ethanol. (B) Half cross-sectional image based on a low-resolution MRI scan of a live *A. planci* individual scanned in artificial seawater with 3.5% $MgCl_2$ for relaxation. Both individuals were scanned using a 3D-TSE scanning sequence. AMP: ampulla; AB: air bubble; END: endoskeleton; CS: cardiac stomach; G: gonad; IS: interradial septum; PC: pyloric cecum; PV: Polian vesicle; S: spine.

pyloric ceca using low-resolution scans and the liquid displacement method. In contrast, for the gonads, the low-resolution scans showed higher agreement with the liquid displacement method than with high-resolution scans (Table 2). The limits of agreement were generally narrower in the gonads (due to smaller values) as compared to the pyloric ceca and ranged from ± 0.22 cm^3 to ± 0.43 cm^3 (Table 2). The volumetric data of all comparisons were plotted against each other and a line of equality was added in order to visualize their offset or agreement, respectively (Fig. 2). A standard error of 12.2% and 12.7% was found in the comparison of high-resolution and low-resolution scan volumes for gonads and pyloric ceca. The comparison of volumes from the low-resolution scans and the liquid displacement method revealed standard errors of 14.5% and 16% for gonads and pyloric ceca, respectively. Although high-resolution scans resemble closely the natural shape, low-resolution scans still offer an adequate approximation to the latter (Fig. 3).

3.3. In vivo MRI

The 3D-bFFE scanning sequence did not cause any obvious artifacts, although *C. novaeguineae* and *P. alveolatus* possess a thicker body wall than *A. planci*, with smaller and more densely packed skeletal elements. Pyloric ceca and gonads could be clearly identified in the images. Hence, this sequence is applicable to the starfish species tested and the image stacks obtained are suitable for accurate reconstruction and volume determination of internal organs (Fig. 4). Also the 3D-TSE sequence works well with living starfish (Fig. 1), although the contrast between pyloric ceca and gonads is not as good as with the 3D-bFFE sequence. We could not find any adverse effect of the anesthetization of the animals, even after repeated application.

Table 1
Mean volumes [cm^3] and standard deviations (s.d.) determined from high-resolution and low-resolution scans and by liquid displacement method for gonads and pyloric ceca. Underlying data set can be found in the electronic supplementary material, Table 1.

Method	Organ	N	Mean volume	±s.d.
High-resolution scans	Gonads	31	1.2610	0.4063
Low-resolution scans	Gonads	31	1.1617	0.3615
Liquid displacement method	Gonads	24	1.1979	0.4422
High-resolution scans	Pyloric ceca	25	1.8231	0.6265
Low-resolution scans	Pyloric ceca	25	1.8197	0.6880
Liquid displacement method	Pyloric ceca	20	2.0189	0.8533

3.4. Test for inter-observer variability

All 3D reconstructions from the five observers resulted in similar volumes for the reconstructed organs. A standard error (as a measure of offset between observers; calculated from all observers) of 7.8% and 4.7% was found for the gonads and pyloric ceca, respectively. This is indicative for a low inter-observer variability (raw data can be found in the electronic supplementary material, Table 2). Visible differences in the 3D models (red arrows in Fig. 5) did not result in significant differences between the obtained volumetric data. In the pyloric ceca, these differences were mainly found in the region proximate to the stomach, where the strings of the pyloric ceca merge and where folds of the stomach or the body wall hamper the clear identification of pyloric cecum tissue. Differences in the gonad 3D models can, for example, be seen in Fig. 5C, where a structure was assigned to the gonads that was not identified as such by any other observer. However, this difference in the 3D models was not reflected by the volumetric data (see ESM, Table 2).

4. Discussion

Digital morphology (Budd and Olsson, 2007; Ziegler et al., 2010) is becoming a widespread method and for some species entire 3D atlases are already available online. For instance, Ruffins et al. (2007) produced a 3D atlas for quail development at an isotropic voxel resolution of 40–70 μm^3 using an 11.7 T pre-clinical MRI system. In contrast, Lauridsen et al. (2011) demonstrated that for the imaging of larger species clinical MRI at 1.5 T with 0.125 mm^3 spatial resolution is sufficient to display internal organs. Here, we present a non-invasive method to image and determine morphometric data on starfish in vivo using clinical MRI and subsequent 3D modeling. Our approach can be used to calculate organ indices for single organisms over a long period of time. Moreover, measurements on internal structures can be conducted in laboratory- or field-based catch and release studies. For the latter methods to tag and track starfish are available (Chim and Tan, 2013; Lamare et al., 2009). Furthermore, we show that MRI can also be used in preserved specimens to depict and analyze their morphological features.

4.1. In vivo MRI

Although the two scanning sequences used in this study, 3D-TSE and 3D-bFFE, can theoretically be applied both in living and preserved starfish, we suggest to employ the latter for scanning living individuals, as it offers better contrast and less sensitivity to movement artifacts due to shorter echo times. Slow water movement can occasionally occur during scanning due to the water exchange between the anesthetized starfish and the surrounding medium. This water exchange produces a so-called "outflow-effect", because excited protons are leaving the investigated plane and cannot be detected anymore (Weishaupt et al., 2006). However, such image artifacts only affect the surrounding water and not the image of the starfish itself. To avoid further signal extinctions or scanning artifacts, living specimens should be scanned without stones or rubble inside the container. The anesthetization using $MgCl_2 \times 6H_2O$ was applied to the same starfish at five consecutive days as well as every month over half a year. All individuals were in good condition after recovery from the anesthetization (about 1 h after

Table 2
Mean differences in volumes [cm^3] between measurement methods and limits of agreement ($\pm t \times$ s.d.) for gonads and pyloric ceca. s.d.: standard deviation. T-factors were adapted to the sample size and corresponding to P = 95%. Underlying data set can be found in the electronic supplementary material, Table 1.

Volume difference	Organ	N	Mean difference	±s.d.	t-Factor	$\pm t \times$ s.d.
High-resolution scans − low-resolution scans	Gonads	31	0.0993	0.1086	2.04	0.2215
High-resolution scans − low-resolution scans	Pyloric ceca	25	0.0034	0.1641	2.09	0.3430
Low-resolution scans − liquid displacement method	Gonads	24	0.0069	0.1193	2.09	0.2493
Low-resolution scans − liquid displacement method	Pyloric ceca	20	−0.1240	0.2057	2.09	0.4299

treatment). In cephalopods (Mollusca: Cephalopoda), this anesthetic has also been shown not to cause any negative effects and should be preferred over other available substances (Messenger et al., 1985). In general, scanning in seawater has one disadvantage compared to scanning in freshwater or other liquids: the high amount of paramagnetic ions in this medium influences the signal-to-noise ratio negatively, resulting in a reduced resolution of the produced images. However, lowering the salinity is not feasible, because a notable increase in image quality would result in too much physiological stress for marine organisms (Blackband and Stoskopf, 1990). Replacing $NaCl_2$ with other salts also does not improve image quality significantly and in the same line may interfere with the living specimen (Blackband and Stoskopf, 1990). Therefore, quality loss has to be compensated using longer scan times. So far, quantitative MRI data from zoological specimens has only scarcely been published. Smith and Reddy (2012) found MRI to be a suitable tool to measure the condition index of oysters (comparable to the GI in starfish) used in aquaculture. In a similar way, Goodall et al. (2009) measured the changes in the volume of chick embryo eyes during development in ovo using 3D models based on MRI datasets.

We show that clinical MRI is suitable to depict gonads and pyloric ceca in living starfish adequately and without the use of specialized coils or long scan times. The 3D models generated demonstrate that morphometric parameters of organs, such as shape or volume, can be related to the physical condition or phylogeny of living starfish. Therefore, MRI constitutes a suitable tool to investigate selected internal structures of starfish quantitatively both in vivo as well as ex vivo.

4.2. 3D reconstruction

The process of 3D reconstruction is relatively easy to perform. However, when scanning preserved specimens, the presence of air within the body cavity should be avoided. Air may not only displace organs, but it also produces signal extinctions in its close vicinity. In order to prevent such artifacts, we suggest using the 3D-TSE sequence for preserved specimens, as it is less sensitive to air than the 3D-bFFE sequence. Nonetheless, because air bubbles are pictured in black, they can usually be identified and distinguished from tissues and skeletal elements either through gray-scale contrast or shape (Fig. 1A). In general, most of the tissues were depicted with similar gray-scale values. Thus,

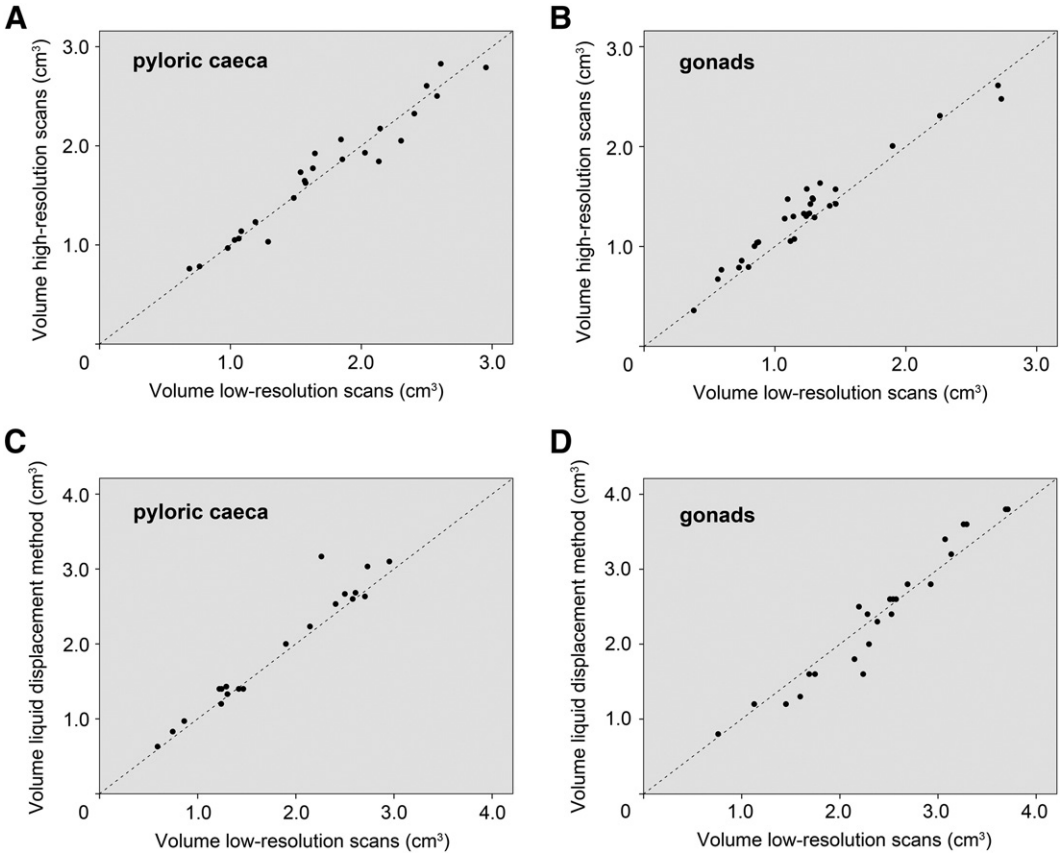

Fig. 2. Volume data obtained from low-resolution scans versus high-resolution scans of the pyloric ceca (A) and gonads (B). Volume data obtained from low-resolution scans versus liquid displacement method for pyloric ceca (C) and gonads (D). Dashed line: line of equality.

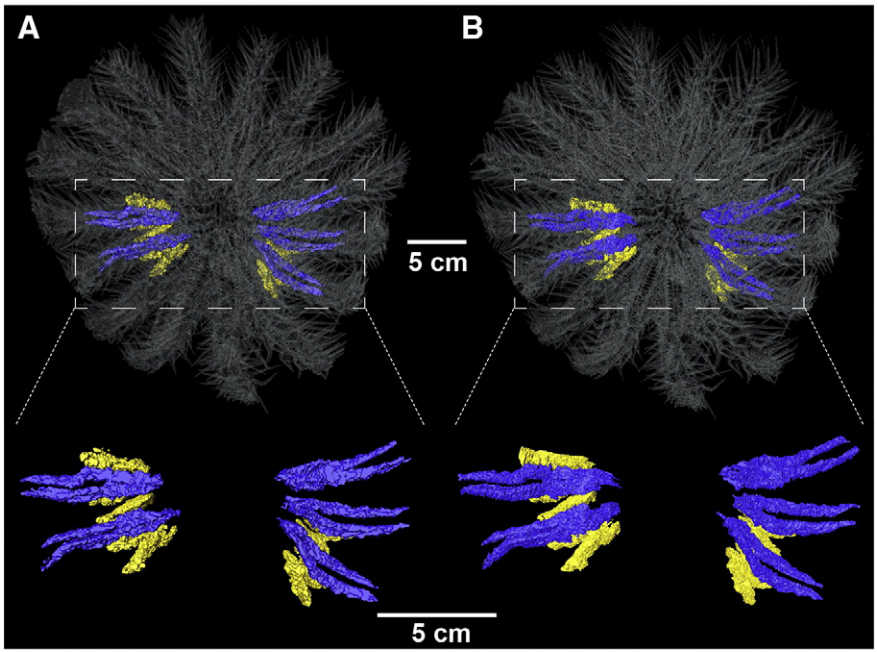

Fig. 3. Exemplarily: 3D models of a single preserved specimen of *A. planci* from which volumes were calculated. (A) Low-resolution scan. (B) High-resolution scan. Top: overview, bottom: selected organs in detail. Blue: pyloric ceca, yellow: gonads, light gray: endoskeleton.

where different tissues are lying close to each other, their differentiation is impeded. For example, gray-scale values assigned to gonads were sometimes difficult to distinguish from the interradial septum in low-resolution scans. In this particular case, the segmented structures were assigned to gonadal tissue. However, in high-resolution scans of preserved specimens interradial septa were clearly visible and contrast was better between gonads and pyloric ceca (Fig. 1A). Due to the lack of sufficient contrast between organs in the high-resolution and the low-resolution scans, the volume cannot be quantified automatically using voxel counts, as previously employed in oysters (Davenel et al., 2010). Contrast could in theory be improved using the variation of sequence weighting, but usually at the expense of signal-to-noise ratio (Benveniste and Blackband, 2002). Therefore, it is currently inevitable to segment the structures of interest by hand in order to produce 3D models for volumetric measurements. Techniques that employ algorithms for automated segmentation could make this process faster and not subject to handwork. Such techniques have already been applied for various purposes, for example in volume renderings of bones (Rodt et al., 2006) or corals (Laforsch et al., 2008) using computed tomography (CT) datasets. The on-going improvement of shape analysis and pattern recognition algorithms in combination with the development of geometric definitions of internal structures might lead to fully automated segmentation algorithms for a variety of animal taxa in the future (Lauridsen et al., 2011). General knowledge on the morphology of starfish will help to clearly identify the structures seen on the low-resolution images and enable the accurate reconstruction when organs lie close to each other and gaps between them cannot be resolved. Nonetheless, 3D reconstructions can be successfully performed even by untrained persons who only received a short introduction to the software as demonstrated by the inter-observer variability test. Although differences occur in 3D reconstructions, these differences are relatively small and do not account for significant variability in the obtained data. A careful revision of all available cutting planes can help to prevent misidentification of tissues, which was a problem especially in the most aboral part of the pyloric ceca, close to the stomach (Fig. 5). Due to their small size (9.8×10^{-5} cm^3 in low-resolution scans) single voxels that are omitted during the segmentation of organs only account for a minimal change in the volume of the whole organ. Furthermore, in order to save time in the process of 3D reconstruction, the volume calculation of one pair of gonads or pyloric ceca within a single arm can already be sufficient to determine the respective organ index (Sanford et al., 2009).

4.3. Comparison of volumetric datasets

The limits of agreement (relative to the mean volumes of both methods together) of high-resolution and low-resolution scans were ±18.3% for gonads and ±18.8% for pyloric ceca. This rather wide range occurred because more anatomical detail can be resolved in high-resolution scans. The structure of interest can therefore be segmented more accurately, resulting in different volumetric data compared to low-resolution scans. The mean volume in high-resolution scans was generally higher than in low-resolution scans. This moderate difference might have emerged due to the applied segmentation workflow. By using the “magic wand” tool, excess voxels are marked that are removed during revision. Due to the larger voxel size in low-resolution scans, a removal of voxels could have caused a larger decline in total volume as in high-resolution scans. However, when determining size or changes in volume using only low-resolution scans as underlying datasets, differences between observers are the crucial factor that accounts for variability in the data: 7.8% and 4.7% for the gonads and pyloric ceca, respectively. Between low-resolution scans and liquid displacement method, the limits of agreement – relative to the mean volumes of both methods together – were broader, with ±21.1% for gonads and ±22.4% for pyloric ceca. This slightly higher variability suggests that the liquid displacement method contains more possible sources of errors in contrast to the MRI-based approach. First, the accuracy of the former method is dependent on the measuring cylinder or the balance used, whose accuracy is again dependent on size or weight of the sample (Hughes, 2005). Second, during dissection, parts may be lost or fluid might leak out of the structures in different quantities. Third, a random error may occur during the measurement process (e.g. draining procedure when measuring wet material, water absorption of the object, absorbed air bubbles; Hughes (2005)). Finally,

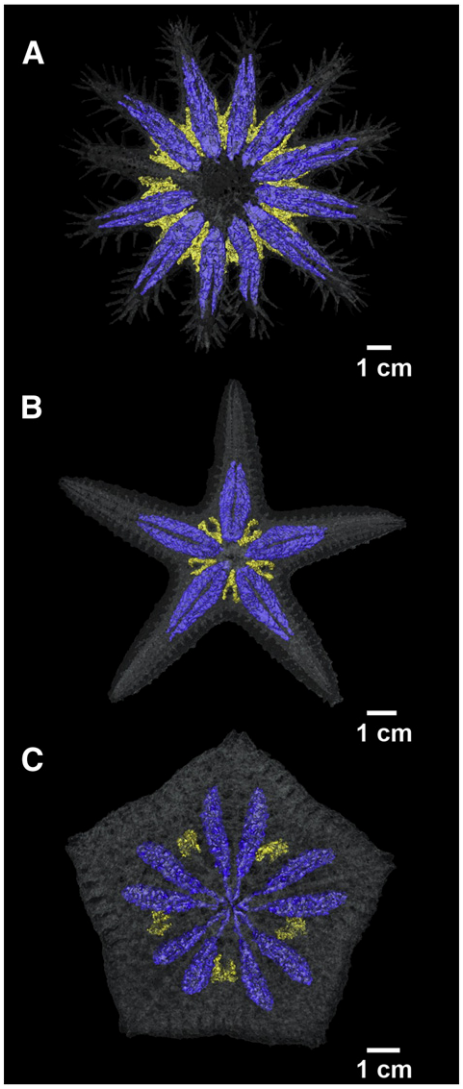

Fig. 4. Aboral views of 3D reconstructions of starfish scanned in vivo. Blue: pyloric ceca, yellow: gonads, light gray: endoskeleton. (A) *A. planci*. (B) *P. alveolatus*. (C) *C. novaeguineae*. Note that the starfish (A) is missing the pyloric ceca in one of its arms.

reading the values may also lead to a random error. However, all conventional methods to obtain quantitative data on internal structures of starfish involve dissection and therefore come with a number of potential sources of error. In contrast, the accuracy of MRI is limited only by resolution. When performing 3D reconstructions, there is a certain amount of variability in the data obtained, but as obvious from our inter-observer tests, a bias of maximally 7.8% will still provide accurate data.

In order to scan whole animals of larger size in vivo, we used clinical MRI at comparatively low resolutions (0.07–0.09 mm^3/voxel for low-resolution scans). This isotropic voxel resolution is sufficient to undertake measurements on organs even if tiny structures such as most parts of the ambulacral system could not be resolved. Although high-resolution scans provide a more realistic impression of the internal anatomy, the applicability of our approach primarily relies on the datasets with lower resolution. Firstly, because editing high-resolution scans is more time-consuming as the amount of sectional planes is larger. Secondly, because the time needed for scanning should be reduced to a minimum in order to reduce stress in living starfish. High-resolution scans took about 10 to 15 h, whereas low-resolution scans were completed in 15 to 20 min. Finally, the reduction of scan time lowers the cost of MRI usage as charges for clinical and pre-clinical MRI systems can be several hundred US-$ per hour (Holliman et al., 2008). By using a low-resolution scan protocol, as suggested here, about three to four large starfish can be scanned per hour, but scan time can vary depending on the sequence chosen. However, scan time can be shortened by using MR scanners with stronger magnet strength (Weishaupt et al., 2006). With the on-going development of clinical MRI, magnet strengths will increase, providing the opportunity of shorter scan times while achieving higher resolutions (Duyn, 2012). Pre-clinical MRI offers such higher field strengths, but the use of these systems is restricted by the size of the sample that can be investigated (usually the diameter of the pre-clinical MRI magnet bore, where the sample is placed, is 3–4 cm or lower) and their limited availability (Ziegler and Müller, 2011; Ziegler et al., 2008; Ziegler et al., 2011). Clinical MRI systems, in contrast, can be found in numerous hospitals around the world (Holliman et al., 2008).

5. Conclusions

Until recently, MRI has only rarely been employed in biological research to obtain quantitative data. Long scan times and the limited availability of pre-clinical MRI systems often impeded such studies. To overcome these obstacles, we used more widely available clinical MRI systems at low resolutions (therefore short scan times) to measure the volume of starfish organs. We found limits of agreement that were rather broad when comparing our method to the conventional liquid displacement method for volume determination and to high resolution scans. However, as discussed above, a consequent use of low-resolution scans will provide accurate data with a bias below 8%. In contrast to previous methodological approaches, the MRI-based method advocated here permits time series analyses of organs in single living specimens. The images produced using MRI provide detailed information about anatomical structures and can therefore also be used for two-dimensional measurements or other anatomical investigations. These in vivo insights alone can, among others, be used to look at the presence or absence of certain organs, and this can be used, for example, in determining an individual's sexual maturity. Additionally, they can display anatomical features or abnormalities, for example missing organs or the status of organs in regenerating body parts. Furthermore, the technique suggested for preserved specimens can be used for morphological and phylogenetic investigations.

MRI protocols have already been developed for a wide range of animal taxa, which permits our approach to be applied to other animal groups in order to obtain volumetric data from internal structures in vivo. This holds especially true for other echinoderm classes such as sea urchins (Echinodermata: Echinoidea) or sea cucumbers (Echinodermata: Holothuroidea) where our approach should be applicable with only minor adaptations.

Acknowledgments

We thank Felicitas Buchberger, Fernanda Fadel and Anastasia DeMotte for performing the 3D reconstructions for the inter-observer variability test and Mechthild Kredler for ideas and help during the experiments. Financial support for Robert Sigl by the Cusanuswerk and for Hannes Imhof by the Studienstiftung des deutschen Volkes is gratefully acknowledged. We would like to thank three anonymous reviewers for their valuable comments. **[RH]**

Appendix A. Supplementary data

Supplementary data to this article can be found online at http://dx.doi.org/10.1016/j.jembe.2013.08.002.

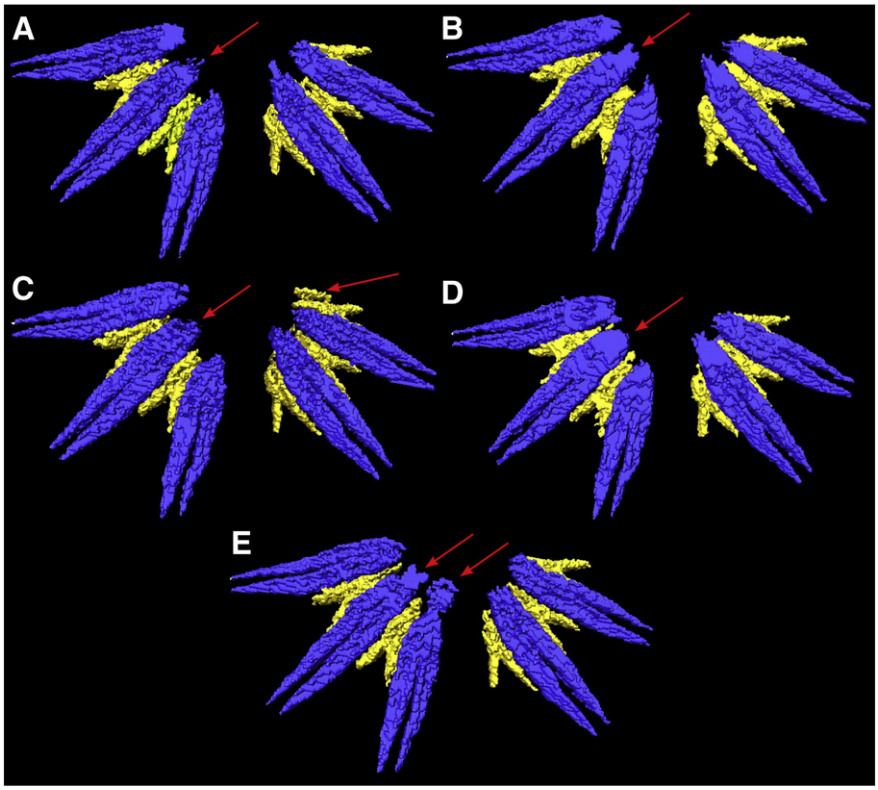

Fig. 5. Reconstructed pyloric ceca and gonads from the inter-observer variability test using the same MRI scan from a single living specimen of *Acanthaster planci*. This test was performed by five different observers (A)–(E). Red arrows indicate differences in reconstructed organ shapes exemplarily.

References

Benveniste, H., Blackband, S., 2002. MR microscopy and high resolution small animal MRI: applications in neuroscience research. Prog. Neurobiol. 67, 393–420.

Birkeland, C., Lucas, J., 1990. *Acanthaster planci*: Major Management Problem of Coral Reefs. CRC Press, Boca Raton.

Blackband, S., Stoskopf, M.K., 1990. In vivo nuclear magnetic resonance imaging and spectroscopy of aquatic organisms. Magn. Reson. Imaging 8, 191–198.

Bland, J.M., Altman, D.G., 1986. Statistical methods for assessing agreement between two methods of clinical measurement. Lancet 1, 307–310.

Bland, J.M., Altman, D.G., 2003. Applying the right statistics: analyses of measurement studies. Ultrasound Obstet. Gynecol. 22, 85–93.

Boistel, R., Swoger, J., Kržič, U., Fernandez, V., Gillet, B., Reynaud, E., 2011. The future of three-dimensional microscopic imaging in marine biology. Mar. Ecol. 32, 438–452.

Budd, G., Olsson, L., 2007. Editorial: a renaissance for evolutionary morphology. Acta Zool. 88, 1.

Chia, F., Koss, R., 1994. Asteroidea. In: Harrison, F., Chia, F. (Eds.), Microscopic Anatomy of Invertebrates. Wiley-Liss, New York, pp. 169–245.

Chim, C.K., Tan, K.S., 2013. A method for the external attachment of acoustic tags on sea stars. J. Mar. Biol. Assoc. U. K. 93, 267–272.

Dare, P., 1982. Notes on the swarming behaviour and population density of *Asterias rubens* L. (Echinodermata: Asteroidea) feeding on the mussel, *Mytilus edulis* L. J. Conseil 40, 112–118.

Davenel, A., González, R., Suquet, M., Quellec, S., Robert, R., 2010. Individual monitoring of gonad development in the European flat oyster *Ostrea edulis* by in vivo magnetic resonance imaging. Aquaculture 307, 165–169.

Duyn, J.H., 2012. The future of ultra-high field MRI and fMRI for study of the human brain. NeuroImage 62, 1241–1248.

Ebert, T.A., Hernandez, J.C., Russell, M.P., 2011. Problems of the gonad index and what can be done: analysis of the purple sea urchin *Strongylocentrotus purpuratus*. Mar. Biol. 158, 47–58.

Farmanfarmaian, A., Giese, A.C., Boolootian, R.A., Bennett, J., 1958. Annual reproductive cycles in four species of west coast starfishes. J. Exp. Zool. 138, 355–367.

Freeman, S.M., Richardson, C.A., Seed, R., 2001. Seasonal abundance, spatial distribution, spawning and growth of *Astropecten irregularis* (Echinodermata: Asteroidea). Estuar. Coast. Shelf Sci. 53, 39–49.

Goodall, N., Kisiswa, L., Prashar, A., Faulkner, S., Tokarczuk, P., Singh, K., et al., 2009. 3-Dimensional modelling of chick embryo eye development and growth using high resolution magnetic resonance imaging. Exp. Eye Res. 89, 511–521.

Hamel, J., Mercier, A., 1995. Prespawning behavior, spawning, and development of the brooding starfish *Leptasterias polaris*. Biol. Bull. 188, 32–45.

Hayek, L.A.C., Buzas, M.A., 2010. Surveying Natural Populations: Quantitative Tools for Assessing Biodiversity. Columbia University Press, New York (41 pp.).

Holliman, M.F., Davis, D., Bogan, A.E., Kwak, T.J., Gregory Cope, W., Levine, J.F., 2008. Magnetic resonance imaging of live freshwater mussels (Unionidae). Invertebr. Biol. 127, 396–402.

Hughes, S.W., 2005. Archimedes revisited: a faster, better, cheaper method of accurately measuring the volume of small objects. Phys. Educ. 40, 468–474.

Jangoux, M., 1982. Digestive systems: Asteroidea. In: Jangoux, M., Lawrence, J. (Eds.), Echinoderm Nutrition. AA Balkema, Rotterdam, pp. 235–272.

Kaandorp, J.A., Sloot, P.M.A., Merks, R.M.H., Bak, R.P.M., Vermeij, M.J.A., Maier, C., 2005. Morphogenesis of the branching reef coral *Madracis mirabilis*. Proc. R. Soc. B 272, 127–133.

Laforsch, C., Christoph, E., Glaser, C., Naumann, M., Wild, C., Niggl, W., 2008. A precise and non-destructive method to calculate the surface area in living scleractinian corals using X-ray computed tomography and 3D modeling. Coral Reefs 27, 811–820.

Laforsch, C., Imhof, H., Sigl, R., Settles, M., Heß, M., Wanninger, A., 2012. Applications of computational 3D-modeling in organismal biology. In: Alexandru, C. (Ed.), Modeling and Simulation in Engineering. InTech, pp. 117–142.

Lamare, M.D., Channon, T., Cornelisen, C., Clarke, M., 2009. Archival electronic tagging of a predatory sea star — testing a new technique to study movement at the individual level. J. Exp. Mar. Biol. Ecol. 373, 1–10.

Lauridsen, H., Hansen, K., Wang, T., Agger, P., Andersen, J.L., Knudsen, P.S., et al., 2011. Inside out: modern imaging techniques to reveal animal anatomy. PLoS One 6, e17879.

Lawrence, J., 1973. Level, content, and caloric equivalents of the lipid, carbohydrate, and protein in the body components of *Luidia clathrata* (Echinodermata: Asteroidea: Platyasterida) in Tampa Bay. J. Exp. Mar. Biol. Ecol. 11, 263–274.

Lawrence, J., Lane, J.M., 1982. The utilization of nutrients by post-metamorphic Echinoderms. In: Jangoux, M., Lawrence, J. (Eds.), Echinoderm Nutrition. AA Balkema, Rotterdam, pp. 331–371.

Loosanoff, V., 1964. Variations in time and intensity of setting of the starfish, *Asterias forbesi*, in Long Island Sound during a twenty-five-year period. Biol. Bull. 126, 423–439.

Mariante, F.L.F., Lemos, G.B., Eutrópio, F.J., Castro, R.R.L., Gomes, L.C., 2010. Reproductive biology in the starfish *Echinaster* (*Othilia*) *guyanensis* (Echinodermata: Asteroidea) in southeastern Brazil. Zoologia (Curitiba) 27, 897–901.

Matre, K., Stokke, E.M., Martens, D., Gilja, O.H., 1999. In vitro volume estimation of kidneys using three-dimensional ultrasonography and a position sensor. Eur. J. Ultrasound 10, 65–73.

Mauzey, K.P., 1966. Feeding behavior and reproductive cycles in *Pisaster ochraceus*. Biol. Bull. 131, 127–144.

Menge, B., 1972. Competition for food between two intertidal starfish species and its effect on body size and feeding. Ecology 53, 635–644.

Menge, B., 1974. Effect of wave action and competition on brooding and reproductive effort in the seastar, *Leptasterias hexactis*. Ecology 55, 84–93.
Messenger, J.B., Nixon, M., Ryan, K.P., 1985. Magnesium chloride as an anaesthetic for cephalopods. Comp. Biochem. Physiol. C 82, 203–205.
Paine, R.T., 1969. The *Pisaster–Tegula* interaction: prey patches, predator food preference, and intertidal community structure. Ecology 50, 950–961.
Paine, R.T., 1971. A short-term experimental investigation of resource partitioning in a New Zealand rocky intertidal habitat. Ecology 52, 1096–1106.
Rodt, T., Bartling, S.O., Zajaczek, J.E., Vafa, M.A., Kapapa, T., Majdani, O., et al., 2006. Evaluation of surface and volume rendering in 3D-CT of facial fractures. Dentomaxillofac. Rad. 35, 227–231.
Ruffins, S.W., Martin, M., Keough, L., Truong, S., Fraser, S.E., Jacobs, R.E., Lansford, R., 2007. Digital three-dimensional atlas of quail development using high-resolution MRI. TheScientificWorldJOURNAL 7, 592–604.
Sanford, E., Wood, M.E., Nielsen, K.J., 2009. A non-lethal method for estimation of gonad and pyloric caecum indices in sea stars. Invertebr. Biol. 128, 372–380.
Smith, P., Reddy, N., 2012. Application of magnetic resonance imaging (MRI) to study the anatomy and reproductive condition of live Sydney rock oyster, *Saccostrea glomerata* (Gould). Aquaculture 334–337, 191–198.
Turk, T., Zahl, S., Van Belle, G., Zeisig, T., 1978. QUERY: testing the effect of an intervention in sequential ecological data. Biometrics 34, 128–137.
Weishaupt, D., Köchli, V., Marincek, B., 2006. How Does MRI Work. An Introduction to the Physics and Function of Magnetic Resonance Imaging. Springer, Heidelberg (32 pp.).
Yasuda, N., Ogasawara, K., Kajiwara, K., Ueno, M., Oki, K., Taniguchi, H., et al., 2010. Latitudinal differentiation in the reproduction patterns of the crown-of-thorns starfish *Acanthaster planci* through the Ryukyu Island Archipelago. Plankon Benthos Res. 5, 156–164.
Ziegler, A., Mueller, S., 2011. Analysis of freshly fixed and museum Invertebrate specimens using high-resolution, high-throughput MRI. In: Schröder, L., Faber, C. (Eds.), In Vivo NMR Imaging. Humana Press, New York, pp. 633–651.
Ziegler, A., Faber, C., Mueller, S., Bartolomaeus, T., 2008. Systematic comparison and reconstruction of sea urchin (Echinoidea) internal anatomy: a novel approach using magnetic resonance imaging. BMC Biol. 6.
Ziegler, A., Ogurreck, M., Steinke, T., Beckmann, F., Prohaska, S., Ziegler, A., 2010. Opportunities and challenges for digital morphology. Biol. Direct 5, 1–9.
Ziegler, A., Kunth, M., Mueller, S., Bock, C., Pohmann, R., Schröder, L., et al., 2011. Application of magnetic resonance imaging in zoology. Zoomorphology 130, 227–254.